In Vivo Single-Molecule Dynamics of Transcription of the Viral T7 Phi 10 Promoter in *Escherichia coli*

Nadia S.M. Goncalves[1], Huy Tran[1], Samuel M.D. Oliveira[1], Ramakanth Neeli-Venkata[1], Andre S. Ribeiro[1]
[1] Laboratory of Biosystem Dynamics, Tampere University of Technology, Finland.
e-mail: andre.ribeiro@tut.fi

Leonardo Martins[2], José M. Fonseca[2]
[2]Computational Intelligence Group, CTS/UNINOVA, Faculdade de Ciências e Tecnologia da Universidade Nova de Lisboa, Portugal.
e-mail: jmf@uninova.pt

***Abstract* – We study the dynamics of transcription initiation of the T7 Phi 10 promoter as a function of temperature, using quantitative polymerase chain reaction (qPCR) and *in vivo* single-cell, single-ribonucleic acid (RNA) time-lapse microscopy. First, from the mean and squared coefficient of variation of the empirical distribution of intervals between consecutive RNA appearances in individual cells, we find that both the mean rate and noise in RNA production increase with temperature (from 20ºC to 43ºC). Next, the process is shown to be sub-Poissonian in all conditions, suggesting the existence of more than one rate-limiting step and absence of a significant ON-OFF mechanism. Next, from the kinetics of RNA production for varying amounts of T7 RNA polymerases, we find that as temperature increases, the fraction of time that the T7 RNA polymerase spends in open complex formation increases relative to the time to commit to closed complex formation, due to changes in the kinetics of open complex, closed complex, and reversibility of the closed complex formation. We conclude that the initiation kinetics of the T7 Phi 10 promoter changes with temperature due to changes in the kinetics of its rate-limiting steps.**

Keywords – Transcription; Open and closed complex formation; T7 Phi 10 promoter

I. INTRODUCTION

The bacteriophage T7 is an obligate lytic phage that infects *Escherichia coli*, using the host system to produce up to 100 progeny phages in less than 25 min, in optimal conditions [1]. One of the major gene products of T7 bacteriophage is the T7 RNA polymerase (T7 RNAP) [2]. This is a single subunit enzyme, with a high specificity towards T7 promoters via the recognition of a highly conserved 23bp consensus sequence [3]. Early studies have shown that the T7 RNAP transcription rate is sequence dependent and depends on environmental conditions [4][5][6]. Given that the infection process of T7 bacteriophage is not only fast but it also requires a balance between the number of phages and the amount of capsid proteins produced [7], the phage needs to coordinate the dynamics of transcription of the viral genes, as this is likely critical for its success.

It is known that the dynamics of gene expression, as well as of many other cellular processes, depends on environmental factors, particularly temperature [8]. Consequently, microorganisms have evolved mechanisms that allow them to cope with both sudden as well as slow temperature changes [9][10]. *E. coli*, for example, can survive in a wide range of temperatures. Similarly, it has also been shown that the T7 bacteriophage is capable of coping with these fluctuations and wide ranges [5].

Even though robustness to sudden temperature changes and wide temperature ranges is crucial for the survival of microorganisms, so far, little is known about what are the consequences of these environmental changes on the *in vivo* transcription kinetics of the T7 promoter. In addition, most studies characterizing the transcription initiation kinetics of T7 promoters have mostly used *in vitro* measurement techniques [5][11].

To address this issue, here we use recently developed measurement strategies that use single-cell, single-RNA *in vivo* detection techniques [12] and use them to study in detail the kinetics of transcription initiation of the T7 *Phi10* (*Φ10*) promoter as a function of temperature.

The remaining of this article is organized as follows: Section II describes the methods used and measurements conducted. Section III presents the results from these experiments. In Section IV, we conclude by presenting our interpretation of the results and our assessment of their relevance, as well as additional considerations for future work.

II. METHODS

In this section, we describe the measurements conducted in this study. Each subsection presents a detailed explanation of the experiments performed.

A. Strain and plasmids

The strain *E. coli* BL21(DE3) (New England Biolabs, USA) was used to express the target and reporter genes. This strain has a copy of the T7 bacteriophage gene 1 coding for T7 RNAP controlled by the P_{lacUV5} promoter and integrated in the chromosome [13] (Figure 1A).

The single copy F-plasmid pBELOBAC11, carrying the *Φ10-mCherry-48bs* sequence (constructed for this work) was inserted in the host strain. It produces the target RNA, with an array of 48 MS2 binding sites (*48bs*) under the control of a T7 *Φ10* promoter, cloned from the plasmid pRSET/EmGFP (ThermoScientific, USA).

A second plasmid, pZA25-GFP (Green Fluorescent Protein) [14] (a gift from Orna Amster-Choder, Hebrew University of Jerusalem, Israel), was also inserted in the host strain. It contains the reporter gene *ms2-gfp*, placed under the control of P_{BAD} promoter. This reporter gene encodes for the fusion protein MS2-GFP, which binds the target RNAs and renders them visible as bright spots under the confocal microscope [15] (Figure 1B). From here onwards we refer to the T7 *Φ10* promoter as T7 promoter.

 ISBN: 978-1-61208-488-6

B. Microscopy

For live cell microscopy, BL21(DE3) cells were incubated in M63 medium supplemented with Glucose (0.4%) and the appropriate concentration of Chloramphenicol and Kanamycin (Sigma Aldrich, USA) and was grown overnight at 30°C, with shaking (250 rpm). Cells from the overnight culture were then diluted in fresh M63 medium, with an initial OD600 ~ 0.05, and incubated at 37°C, for 90 minutes with shaking (250 rpm). Then, cells were pelleted and re-suspended in ~100 μl of M63 medium. Four microliters of cells were placed between a 3% agarose gel pad, made with M63 medium, and a glass coverslip before assembling the imaging chamber (CFCS2, Bioptechs, USA). Two hours before the microscopy measurements, a flow of fresh M63 medium at 37°C containing the reporter inducer (0.8% L-arabinose) was initiated with a peristaltic pump at a rate of 1 ml/min to produce sufficient MS2-GFP molecules in the cells to detect the target RNA in all experiments. Note that we shifted the temperature in the chamber from 37°C to 20°C or to 43°C (depending on the condition studied), 20 minutes prior to inducing the target system.

To activate the target system, we induced the production of T7 RNAP, controlled by P_{lacUV5}, by introducing a new flow (1 ml/min) of M63 medium containing 0.8% L-arabinose and Isopropyl β-D-1-thiogalactopyranoside (IPTG) at various concentrations (see below). Once synthesized, T7 RNAPs will bind the T7 promoter and transcribe *48bs* RNAs, which are quickly bound by MS2-GPF molecules and appear under the confocal microscope as bright spots (Figure 1B).

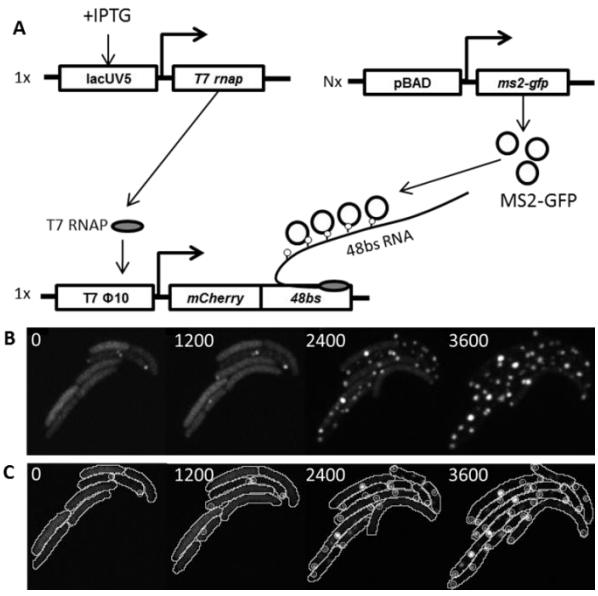

Figure 1. (A) Diagram of the measurement system, depicting the target and reporter genes along with the MS2-GFP tagging process. (B) Confocal microscope images at subsequent time points showing the cells and the MS2-GFP tagged RNA molecules inside. (C) Segmented cells and RNA spots within.

Cells imaging was started at the same time as the introduction of the flow containing IPTG. Images were captured every minute for 2 hours using an inverted microscope Nikon Eclipse (Ti-E, Nikon, Japan). Both confocal images (confocal C2+ scanner connected to LU3 laser system, Nikon) and phase contrast images (DS-Fi2 CCD-camera) were collected.

Examples of confocal images of cells are shown in Figure 1B. Note that, at the end of the time series, the fluorescent background in some cells becomes dimmed due to the produced RNAs having bound most MS2-GFP molecules in the cytoplasm.

C. Image analysis

The segmentation of cells and detection of RNA spots were performed by the software "iCellFusion" [16]. It first applies the cell segmentation on phase contrast images using a Gradient Path Labelling Algorithm [17]. Then, it performs the inter-modal image registration between phase-contrast images and the corresponding fluorescence images and exports the segmentation results on fluorescence images. The spot detection was performed as in [18]. Results from the segmentation and spot detection algorithms are shown in Figure 1C.

D. Data analysis

The cell-to-cell variability in the kinetics of intake of IPTG, which affects the activation of P_{lacUV5} [19][20], creates extrinsic variability regarding when the first RNA appears in each cell. Since we are only interested in the intrinsic noise of the transcription process, to correct for this, we fit the total spot intensity in each cell over time with an activation function:

$$x(t_{activation}, c, t) = c \times H(t - t_{activation}) \times (t - t_{actiovation}) \quad (1)$$

where t is time, $t_{activation}$ is activation time of T7 when the *48bs* RNA production reaches steady state, c is the mean increment rate of total spot intensity and H is a unit step function. With the function in (1) fitted using least mean squared, we find $t_{activation}$ for each cell. The total spot intensities are then aligned using the inferred $t_{activation}$, so as to compare the kinetics of active T7 promoters in individual cells.

We found by inspection that, at 37°C, in the first ~18 minutes, the mean curve of the aligned total spot intensities can be well fitted with a linear function, indicating that RNA production in most cells reached a steady state after their corresponding $t_{activation}$. After the 18th minute, the mean spot intensity increases with decreasing speed, visibly due to increasing shortage of free MS2-GFP. Therefore, for this condition, we select the data in the first 18 minutes for RNA quantification as in [18][21]. Note also that for different temperatures and IPTG concentrations, the window for RNA quantification differs (data not shown).

E. qPCR

Cells grown to OD600 ~0.4 were induced with the appropriate IPTG concentration (5-250 μM) for 1 hour, at the specific temperature (20°C, 37°C and 43°C). Afterwards, cells were fixed with RNAprotect bacteria reagent (Qiagen, Germay), followed by total RNA isolation, DNase I treatment (ThermoScientific, USA) and cDNA

 ISBN: 978-1-61208-488-6

synthesis (BioRad, USA). The qPCR master mix contained iQ SYBR Green supermix (Biorad, USA) with primers for the target gene, the T7 RNAP and the reference gene at a final concentration of 200 nM. The primers for the target gene were (Forward: 5' CACCTACAAGGCCAAGAAGC 3' and Reverse: 5' TGGTGTAGTCCTCGTTGTGG 3') for the mCherry region. To quantify the T7 RNAP, the primers used were (Forward: 5' TCCTGAGGCTCTCACCGC 3' and Reverse: 5' GATACGGCGAGACTTGCGA 3'). For the reference gene 16SrRNA, the primers were (Forward: 5' GCTACAATGGCGCATACAAA 3' and Reverse: 5' TT CATGGAGTCGAGTTGCAG 3'). The data from CFX Manager TM Software was used to obtain the relative gene expression and standard error [22].

F. Model of T7 promoter transcription kinetics

To study how the kinetics of the T7 promoter changes with temperature, we assume the modelling strategy of transcription proposed in [23][24][25], derived from both *in vitro* and *in vivo* studies on viral [11][26] and *E. coli* promoters [8][25][27][28][29]. The model of transcription kinetics of T7 promoter is as follows:

$$R + Pr \underset{k'_{cc}}{\overset{k_{cc}}{\rightleftarrows}} Pr_{cc} \xrightarrow{k_{oc}} Pr_{oc} \xrightarrow{\infty} Pr + R + RNA \quad (2)$$

where R is an active T7 RNAP, Pr is a free promoter, Pr_{cc} is a fully formed closed complex, and Pr_{oc} is a fully formed open complex. The closed complex formation occurs at the rate k_{cc}. Once the closed complex is formed, the promoter can either be unbound by the R at the rate k'_{cc} or undergo open complex formation at the rate k_{oc}. Due to fast promoter escape [30], the low frequency of abortive initiation [6] and the fast rate of elongation of T7 RNAP [5][11][31], we assume that the RNAP and target RNA are released soon after completion of the open complex. Note that this model does not include an ON-OFF mechanism since T7 is a constitutive promoter.

From (2), the mean of the interval distribution (Δt) between consecutive transcription events is:

$$\Delta t(R) = \frac{(k'_{cc} + k_{oc})}{R k_{cc} k_{oc}} + \frac{1}{k_{oc}} = \frac{1+K}{R k_{cc}} + \frac{1}{k_{oc}} = \tau(R) + \tau_{oc} \quad (3)$$

where R is the abundance of T7 RNAP in the cell, K is ratio between k'_{cc} and k_{oc} indicating the reversibility of the closed complex, $\tau(R)$ is the time for an RNAP to commit to the open complex formation, and τ_{oc} is time for open complex formation. From (3), the production interval $\Delta t(R)$ is a linear function of the inverse of T7 RNAP level ($1/R$), and thus:

$$\tau_{oc} = \Delta t(R = \infty) \quad (4)$$

With each set of values of $R.k_{cc}$, K, and k_{oc}, we use the Chemical Master Equation (CME) to find the distribution of intervals between consecutive RNA production events, from which the mean rate and noise in transcription are extracted.

III. RESULTS

This section comprises the results, obtained from the measurements, which are presented into three separate subsections.

A. Validation of the construct with the T7 promoter

First, to validate that the T7 promoter inserted in the F-plasmid (Methods) is active, we measured the RNA levels of the T7 RNAP and of the target gene by qPCR for varying IPTG concentrations (which control the expression of T7 RNAP). Results are shown in Figure 2.

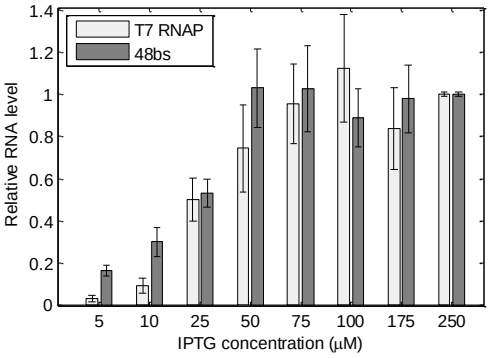

Figure 2. Relative RNA levels of T7 RNAP (light grey) and target gene (*48bs*) (dark grey) at 37°C with varying IPTG concentrations as measured by qPCR. Also shown for each condition are the standard errors from 3 technical replicates.

From Figure 2, first, both the T7 RNAP's and target gene's levels do not increase significantly with increasing IPTG concentrations beyond 100 μM, suggesting that the lacUV5 promoter is fully induced at this concentration. In Figure 2, the data is normalized by the RNA levels at 250 μM IPTG. We validated these measurements, in the case of the target RNA, by observing its production dynamic at 175 μM, 250 μM and 1000 μM IPTG at 37°C under the microscope (via MS2-GFP tagging, Methods).

While we observed changes in the mean activation time of the T7 promoter with changing IPTG concentration (data not shown), we did not observe a significant change in mean transcription rate ($\mu_{\Delta t}$ ~350 s).

Finally, we find an increase in both the T7 RNAP's and target gene's RNA expression with increasing IPTG concentration, demonstrating that both genes are active. Note the close correlation between the activities of the two genes, indicating that the T7 promoter is, as expected, under the control of the T7 RNAP.

B. T7 promoter dynamics at various temperatures

We next observed the transcription dynamics of T7 promoter at different temperatures (within sub-optimal intervals). The IPTG concentration used was 250 μM, in order to ensure that lacUV5 is fully induced in all conditions. Under the microscope, all cells appeared to grow normally, with reduced division rates at lower temperatures. In particular, cells' mean doubling times were 50 min, 60 min and 100 min at 43°C, 37°C and 20°C respectively.

 ISBN: 978-1-61208-488-6

From the RNA numbers over time in individual cells as observed by microscopy at different temperatures, we extracted the mean duration (μ) and coefficient of variation squared (CV^2) of the intervals between consecutive RNA appearances in individual cells as in [18][32]. Results are shown in Table I.

For each temperature, the number of cells observed, the number of samples collected (intervals between consecutive RNAs in individual cells), and the mean and CV^2 of the intervals between consecutive RNA appearances in individual cells are shown. The final column shows the relative RNA levels of T7 RNAP measured by qPCR (normalized by RNA levels at 37°C).

TABLE I. *IN VIVO* TRANSCRIPTION INITIATION DYNAMICS OF THE *T7* PROMOTER AT DIFFERENT TEMPERATURES MEASURED BY MS2-GFP TAGGING OF RNA.

T (°C)	No. Cells	No. Samples	μ (s)	CV^2 (σ^2/μ^2)	Relative T7 RNAp no.
43	150	508	320	0.95	0.86
37	111	311	352	0.85	1
20	68	105	518	0.62	0.46

From Table I, somewhat surprisingly but in agreement with a previous observation by *in vitro* methods [5], the mean length of the RNA production intervals, μ, increases with decreasing temperature. Overall, this indicates that the *in vivo* kinetics of transcription initiation of the T7 promoter is temperature dependent.

Notably, the mean transcription rates *in vivo* are approximately one order of magnitude smaller than those reported from *in vitro* tests [5][11]. This weaker activity in live cells is likely due to the more limited amount of T7 RNAP (bound by the limits in lacUV5's activity) and limited resources (ATP, ribonucleotides, etc.) in the host cells to support the viral transcription process.

Also in Table I, the noise in transcription (as measured by CV^2) decreases with decreasing temperature. A previous work reported a similar result for P_{tetA}, a native promoter of *E. coli* [8].

In addition, in all conditions, the RNA production appears to be a sub-Poissonian process ($CV^2<1$). This suggests that it consists of multiple rate-limiting steps rather than being dominated by an ON-OFF process [11]. Similar *in vivo* sub-Poissonian dynamics of transcription has been observed in several *E. coli* promoters, native and synthetic, when under full induction [8][28][33].

Overall, the results suggest that the process of transcription initiation of the T7 promoter by the T7 RNAP is similar to that of *E. coli* native promoters.

Meanwhile, from the relative numbers of T7 RNAP as measured by qPCR, we find that unlike when controlling with IPTG concentrations, the kinetics of RNA production of the target promoter T7 no longer follows solely the T7 RNAP numbers, as its production rate is not maximized at 37°C while T7 RNAP numbers are. Therefore, we conclude that the observed changes in the T7 promoter dynamics are due to changes in both the kinetic rates of T7 transcription and in T7 RNAP numbers.

C. Estimation of kinetic rates of the T7 promoter

We searched for changes in the underlying kinetics of transcription initiation of the T7 promoter (i.e. in the duration of the closed and open complex formation) with temperature that can explain the changes in the target RNA production with changing temperature.

To quantify how the kinetic rates of T7 promoter evolve with temperature, we followed the strategy proposed in [12] by investigating, for each temperature, how the transcription activity on T7 promoter is affected by the T7 RNAP abundance. This abundance should affect the kinetics of the closed complex formation, but not that of the steps following the closed complex [12].

Here, the T7 RNAP levels, varied by employing different IPTG concentrations (5 μM, 10 μM, 25 μM, 50 μM and 250 μM), and the T7 promoter's activity are measured relatively by qPCR. From these, we infer what would be the relative rate of RNA production given an infinite amount of T7 RNAP in cells (Methods). This rate should correspond to the fraction of time of the transcription initiation process that corresponds to the open complex formation alone [12]. Results for each temperature condition are shown in 'τ plots' in Figure 3.

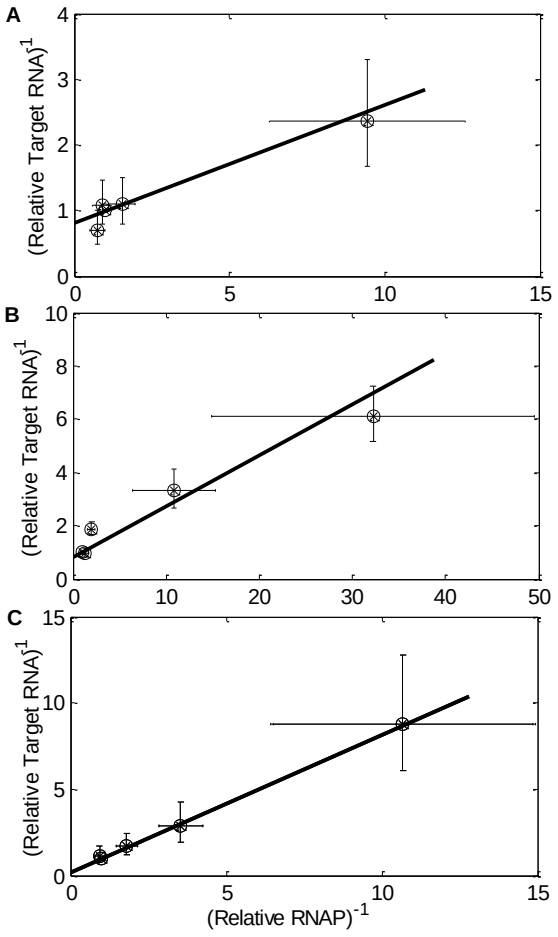

Figure 3. τ plots for T7 promoter activity at different temperatures: (A) 43°C (B) 37°C and (C) 20°C.

In Figure 3, the data is shown relative to the RNA and RNAP levels at 250 μM IPTG. Error bars represent the

standard error of the mean (SEM) of the estimate of the inverse of the relative rates of transcription for the target RNA and T7 RNAP in each condition. The lines are Weighted Total Least Squares fits [34]. Errors are calculated including the uncertainty in the 250 μM IPTG condition in the plot (thus removing the error from that point). From Figure 3, the ratio between the inverse of the T7 RNA production rate for infinite T7 RNAP numbers in the cells (R^{-1}=0) equals 0.82 at 43°C, 0.81 at 37°C, and 0.21 at 20°C. These numbers correspond also to the ratio between open complex formation (τ_{oc}) and mean transcription interval (Δt), described in Table I (Methods).

Next, from the ratio (τ_{oc} /Δt), we calculated the rate of open complex formation (k_{oc}). Given the value of k_{oc}, we can find the values of k_{cc} and K to achieve the same mean and noise (with 95% accuracy) of the transcription intervals shown in Table I (Methods). Results are shown in Table II. Shown are the rate of open complex formation (k_{oc}), the reversibility of the closed complex formation (K) and the rate of closed complex formation ($R.k_{cc}$), given the empirical values of the ratio ($\tau_{oc}/\Delta t$) extracted from Figure 3.

TABLE II. ESTIMATION OF THE KINETIC RATES OF THE T7 PROMOTER INITIATION PROCESS VERSUS TEMPERATURE.

T (°C)	$\tau_{oc}/\Delta t$	k_{oc} (s^{-1})	K	$R.k_{cc}$ (s^{-1})
43	0.822	263^{-1}	> 2.00	$> 20^{-1}$
37	0.808	284^{-1}	1.2±0.5	$(32±8)^{-1}$
20	0.206	107^{-1}	<0.11	$(351±77)^{-1}$

From Table II, the formation of the open complex, following the T7 RNAP commitment to the closed complex, is faster at 20°C and slower at 37°C and 43°C. This seemingly counterintuitive response suggests that, at higher temperatures, the open complex may be less stable and that, has a consequence, it becomes more reversible to the previous state rather than to committing to the elongation complex.

Namely, the reversibility of the closed complex (K) increases with increasing temperature. At 43°C, the closed complex appears to be highly unstable and T7 RNAP likely binds and unbinds from the T7 promoter several times before being able to form a stable open complex, thus reducing the rate of RNA production. At 37°C, the closed complex appears to be more stable, with a ~50% chance of the RNAP unbinding. At 20°C, the chance of this RNAP unbinding appears to become negligible, likely due to both more stable closed complex formation and faster rate of open complex formation.

Finally, the rate of closed complex formation ($R.k_{cc}$) becomes slower with decreasing temperature. It should be noted that this rate is highly dependent on lacUV5's strength (which determines R) and therefore is not a property of the natural system. In the future, direct measurements of the relative T7 RNAP protein levels should help revealing the temperature dependence of the closed complex (k_{cc}) of this system.

IV. CONCLUSION AND FUTURE WORK

The T7 bacteriophage has only the lytic cycle. Once infecting an *E. coli* cell, its genes transcription is activated and proceeds uninterruptedly until the replication of the viral DNA it achieved [2]. The dynamics of transcription (mean and noise), should therefore play a key role in the success rate of this process. Consequently, for this process to be successful in temperature-fluctuating environments, the transcription process ought itself to be robust to a wide range of temperature conditions.

To assess this robustness, we observed for the first time the *in vivo* transcription initiation kinetics of the T7 promoter at the single RNA level as a function of temperature. Our results suggest that, as temperature decreases, both the mean rate of RNA production and the noise in this process decrease. This somewhat surprising result appears to be made possible by the stabilization of the closed complex formation at lower temperatures.

Our results are, to some extent, similar to those reported for a natural promoter of *E. coli*, P_{tetA}. Namely, its initiation kinetics is also sub-Poissonian, with two rate-limiting steps, the closed and the open complex, whose duration is temperature dependent [8]. However, in P_{tetA}, the noise increases for decreasing temperature.

At the moment, it is unknown what specificities the configuration or composition of the T7 promoter allow this opposite behavior, but this knowledge should be of value to the future engineering of synthetic genes and circuits with robust behaviors at low temperature conditions. From the evolutionary point of view, such noise reduction with lowering temperatures could be associated with the need of the virus for balancing the numbers of phages and capsid proteins more accurately as their total numbers are reduced due to the lowering of the mean production rate [2][7].

In this regard, note from Table I that the relative increase in the interval between RNA productions as temperature decreases from 37°C to 20°C is smaller than the decrease in T7 RNAP numbers (which here are artificially controlled by the LacUV5 promoter). This suggests that, provided a constant number of T7 RNAP for changing temperature, the mean rate of transcription from the T7 promoter will not decrease heavily for decreasing temperature in this range.

In the future, we will employ the system used here and, among other, make use of different promoters controlling the expression of the T7 RNAP so as to, by comparing the various results, isolate the effects of temperature on the T7 promoter alone. Also, we observed that this system is capable of quickly depleting cells from MS2-GFP. This may allow studying the kinetics of binding and unbinding of MS2-GFP to the target RNA as a function of temperature, which might give insights, e.g., on the process by which viral RNAs are protected from the host degradation mechanisms.

ACKNOWLEDGMENT

Academy of Finland [257603, A.R.]; Vilho, Yrjö and Kalle Väisälä fund of Finnish Academy of Science and Letters [S.O.]; TUT President's Graduate Programme

[R.N.], Portuguese Foundation for Science and Technology (FCT/MCTES) [SFRH/BD/88987/2012, LM] and PTDC/BBB-MET/1084/2012, JMF and ASR] and FCT Strategic Program UID/EEA/00066/203 of UNINOVA, CTS [LM and JMF].

REFERENCES

[1] I. Molineux, "The T7 Group," in *The Bacteriophages*, Second Edi., Oxford: Oxford University Press, pp. 277–301, 2005.

[2] J. Dunn, F. Studier, and M. Gottesman, "Complete nucleotide sequence of bacteriophage T7 DNA and the locations of T7 genetic elements," *J. Mol. Biol.*, vol. 166, 1983, pp. 477-535.

[3] J. L. Oakley, R. E. Strothkamp, a H. Sarris, and J. E. Coleman, "T7 RNA polymerase: promoter structure and polymerase binding," *Biochemistry*, vol. 18, no. 3, 1979, pp. 528–37.

[4] W. T. McAllister and A. D. Carter, "Regulation of promoter selection by the bacteriophage T7 RNA polymerase in vitro," *Nucleic Acids Res.*, vol. 8, no. 20, 1980, pp. 4821–4837.

[5] R. Ikeda, A. Lin, and J. Clarke, "Initiation of transcription by T7 RNA polymerase as its natural promoters," *J. Biol. Chem.*,vol. 267, no. 4, 1992, pp. 2640–2649.

[6] R. A. Ikeda, "The efficiency of promoter clearance distinguishes T7 class II and class III promoters," *J. Biol. Chem.*, vol. 267, no. 16, 1992, pp. 11322–11328.

[7] M. De Paepe and F. Taddei, "Viruses' life history: Towards a mechanistic basis of a trade-off between survival and reproduction among phages," *PLoS Biol.*, vol. 4, no. 7, 2006, pp. 1248–1256.

[8] A.-B. Muthukrishnan, M. Kandhavelu, J. Lloyd-Price, F. Kudasov, S. Chowdhury, O. Yli-Harja, and A. S. Ribeiro, "Dynamics of transcription driven by the tetA promoter, one event at a time, in live Escherichia coli cells," *Nucleic Acids Res.*, vol. 40, no. 17, 2012, pp. 8472–8483.

[9] F. Arsène, T. Tomoyasu, and B. Bukau, "The heat shock response of Escherichia coli," *Int. J. Food Microbiol.*, vol. 55, 2000, pp. 3–9.

[10] K. Yamanaka, "Cold shock response in Escherichia coli," *J. Mol. Microbiol.*, vol. 1, 1999, pp. 193–202.

[11] G. M. Skinner, C. G. Baumann, D. M. Quinn, J. E. Molloy, and J. G. Hoggett, "Promoter binding, initiation, and elongation by bacteriophage T7 RNA polymerase. A single-molecule view of the transcription cycle," *J. Biol. Chem.*, vol. 279, no. 5, 2004, pp. 3239–3244.

[12] J. Lloyd-Price, S. Startceva, J. G. Chandraseelan, V. Kandavalli, N. Goncalves, A. Häkkinen, and A. S. Ribeiro, "Dissecting the stochastic transcription initiation process in live Escherichia coli," *DNA Res.*, 2016, in press.

[13] F. W. Studier and B. A. Moffatt, "Use of bacteriophage T7 RNA polymerase to direct selective high-level expression of cloned genes," *J. Mol. Biol.*, vol. 189, no. 1, 1986, pp. 113–130.

[14] K. Nevo-Dinur, A. Nussbaum-Shochat, S. Ben-Yehuda, and O. Amster-Choder, "Translation-independent localization of mRNA in E. coli," *Science*, vol. 331, no. 6020, 2011, pp. 1081–1084.

[15] I. Golding and E. Cox, "RNA dynamics in live Escherichia coli cells," *Proc. Natl. Acad. Sci,.* vol. 101, no. 31, 2004, pp. 11310-11315.

[16] J. Santinha, L. Martins, A. Häkkinen, J. Lloyd-Price, S. M. D. Oliveira, A. Gupta, T. Annila, A. Mora, A. S. Ribeiro, and J. R. Fonseca, "iCellFusion: Tool for fusion and analysis of live-cell images from time-lapse multimodal microscopy," in *Biomedical image analysis and mining techniques for improved health outcomes, IGI Global*, 2015, pp. 71-99.

[17] A. D. Mora, P. M. Vieira, A. Manivannan, and J. M. Fonseca, "Automated drusen detection in retinal images using analytical modelling algorithms," *Biomed. Eng. Online*, vol. 10, no. 1, 2011, p. 59.

[18] A. Häkkinen, M. Kandhavelu, S. Garasto, and A. S. Ribeiro, "Estimation of fluorescence-tagged RNA numbers from spot intensities.," *Bioinformatics*, 2014, pp. 1–8.

[19] J. Mäkelä, M. Kandhavelu, S. M. D. Oliveira, J. G. Chandraseelan, J. Lloyd-Price, J. Peltonen, O. Yli-Harja, and A. S. Ribeiro, "In vivo single-molecule kinetics of activation and subsequent activity of the arabinose promoter," *Nucleic Acids Res.*, vol. 41, no. 13, 2013, pp. 6544–6552.

[20] H. Tran, S. M. D. Oliveira, N. Goncalves, and A. S. Ribeiro, "Kinetics of the cellular intake of a gene expression inducer at high concentrations," *Mol. Biosyst.*, vol. 11, no. 9, 2015, pp. 2579–2587.

[21] A. Häkkinen and A. S. Ribeiro, "Estimation of GFP-tagged RNA numbers from temporal fluorescence intensity data," *Bioinformatics*, vol. 31, no. 1, 2015, pp. 69–75.

[22] K. J. Livak and T. D. Schmittgen, "Analysis of relative gene expression data using real-time quantitative PCR and the 2(-Delta Delta C(T)) Method," *Methods*, vol. 25, no. 4, 2001, pp. 402–408.

[23] W. McClure, "Rate-limiting steps in RNA chain initiation," *Proc. Natl. Acad. Sci.*, vol. 77, no. 10, 1980, pp. 5634–5638.

[24] H. Buc and W. R. McClure, "Kinetics of open complex formation between Escherichia coli RNA polymerase and the lac UV5 promoter. Evidence for a sequential mechanism involving three steps," *Biochemistry*, vol. 24, no. 11, 1985, pp. 2712–2723.

[25] W. R. Mcclure, "Mechanism and control of transcription initiation in prokaryotes," *Annu. Rev. Biochem.*, vol. 54, 1985, pp. 171–204.

[26] D. K. Hawley and W. R. Mcclure, "Nucleic compilation and analysis of Escherichia coli promoter DNA sequences," *Nucleic Acids Res.*, vol. 11, no. 8, 1983, pp. 2237–2255.

[27] R. Lutz and H. Bujard, "Independent and tight regulation of transcriptional units in Escherichia coli via the LacR/O, the TetR/O and AraC/I1-I2 regulatory elements," *Nucleic Acids Res.*, vol. 25, no. 6, 1997, pp. 1203–1210.

[28] M. Kandhavelu, J. Lloyd-Price, A. Gupta, A.-B. Muthukrishnan, O. Yli-Harja, and A. S. Ribeiro, "Regulation of mean and noise of the in vivo kinetics of transcription under the control of the lac/ara-1 promoter," *FEBS Lett.*, vol. 586, no. 21, 2012, pp. 3870–3875.

[29] E. Bertrand-Burggraf, J. F. Lefèvre, and M. Daune, "A new experimental approach for studying the association between RNA polymerase and the tet promoter of pBR322," *Nucleic Acids Res.*, vol. 12, no. 3, 1984, pp. 1697–1706.

[30] L. M. Hsu, "Promoter clearance and escape in prokaryotes," *Biochim. Biophys. Acta - Gene Struct. Expr.*, vol. 1577, no. 2, 2002, pp. 191–207.

[31] S. L. Heilman-Miller and S. A. Woodson, "Effect of transcription on folding of the Tetrahymena ribozyme," *RNA*, vol. 9, no. 6, 2003, pp. 722–733.

[32] C. Zimmer, A. Häkkinen, and A. S. Ribeiro, "Estimation of kinetic parameters of transcription from temporal single-RNA measurements," *Math. Biosci.*, vol. 271, 2015, pp. 146–153.

[33] M. Kandhavelu, H. Mannerström, A. Gupta, A. Häkkinen,

J. Lloyd-Price, O. Yli-Harja, and A. S. Ribeiro, “In vivo kinetics of transcription initiation of the lar promoter in Escherichia coli. Evidence for a sequential mechanism with two rate-limiting steps,” *BMC Syst. Biol.*, vol. 5, no. 1, 2011, p. 149.

[34] M. Krystek and M. Anton, “A weighted total least-squares algorithm for fitting a straight line,” *Meas. Sci. Technol.*, vol. 19, no. 7, 2008, p. 079801.

 ISBN: 978-1-61208-488-6